The equality $\rho v_x = m_1 J_{1x}$ is derived also from formula (24), from which it follows that ρv_x is independent of the longitudinal coordinate.

As an analysis of formula (25) showed, with increase in c_{10} ($c_{10} > c_{1h}$) or with increase in c_{1h} ($c_{1h} > c_{10}$) for a prescribed flow rate Q, there is, as in the case of a coaxial channel, an increase in the maximum value of v_z due to an increase in the total flow of gas mixture and a shift of the point t_{max} (at which v_z is maximal) towards the surface with a lower value of c_1 due to slowing down of the flow of gas mixture at the evaporation surface.

An analysis of (26) showed that with increase in c_{10} ($c_{10} > c_{1h}$) or c_{1h} ($c_{1h} > c_{10}$) the longitudinal pressure drop for a prescribed Q increases.

An analysis of formulas (25), (26) showed that at the limit c_{10}, $c_{1h} \to 0$ the formulas for the distribution of v_z and p become the known formulas for a one-component gas

$$v_z = \frac{\alpha_{20}}{2\mu} h^2 t (1 - t), \quad p = p_0 - \alpha_{20} z,$$

where $\alpha_{20} = 12\mu Q/(bh^3 n)$.

Thus, recondensation of molecules of one of the components of a binary mixture greatly affects the distributions of the longitudinal pressure drop and the longitudinal component of the mass flow velocity in the channel. The formulas obtained in this paper can be used to describe the flow of binary gas mixtures in variable-temperature channels with small temperature drops [1], where the transport coefficients (dynamic viscosity, diffusion coefficient, thermal conductivity) can be regarded as quantities that are independent of temperature.

LITERATURE CITED

1. A. Meisen, A. J. Bobkowicz, N. E. Cooke, and E. J. Farcas, "The separation of micron-size particles from air by diffusiophoresis," Can. J. Chem. Eng., 49, 449 (1971).
2. L. G. Loitsyanskii, Mechanics of Liquid and Gas [in Russian], third edition, Nauka, Moscow (1970).
3. J. O. Hirschfelder, C. F. Curtiss, and R. B. Bird, Molecular Theory of Gases and Liquids, Wiley (1954).

CALCULATION OF THE INTERACTION OF A LAMINAR BOUNDARY LAYER WITH AN EXTERNAL SUPERSONIC FLOW BEHIND AN OBSTACLE

A. N. Antonov

UDC 532.526.2:533.69.011.5

One can cite many papers dealing with investigation of flows in zones of separation and reattachment of a laminar boundary layer [1-12]. In regard to computational methods, it should be noted that the method of interaction of the boundary layer with an external perfect flow, to determine flows in the base region, was first proposed in [1]. However, the lack of sufficient data on the characteristics of the incompressible laminar boundary layer has made it impossible to obtain satisfactory results on base pressure. In [4, 5] the proposed method was modified and applied to the region of interaction of a density shock with a boundary layer [4], and also in the region of separation of the laminar boundary layer on a cylindrical body in transverse flow [5].

The present paper computes flows behind two-dimensional and axisymmetric obstacles, based on a scheme for interaction of the boundary layer with an external perfect flow.

1. We consider the following approximate flow scheme in the base region behind an obstacle washed by a uniform supersonic stream, a scheme of typical interaction of the boundary layer with an external perfect flow (Fig. 1). Between sections 1 and 2 there is flow expansion, AB is a line of constant mass flux, and B is the stagnation point. The broken line denotes the edge of the boundary layer. Immediately behind the body, between sections 2 and 3, there is a constant-pressure separation region, so that the interaction flow begins at some section 3. The calculation of the interaction between the viscous layers and the external, perfect, almost isentropic stream is carried out, as usual, with the boundary layer equations. We write down the system of equations for the compressible laminar boundary layer

$$\frac{\partial (\rho u)}{\partial x} + \frac{\partial (\rho v)}{\partial y} = 0; \tag{1.1}$$

Moscow. Translated from Zhurnal Prikladnoi Mekhaniki i Tekhnicheskoi Fiziki, No. 3, pp. 56-64, May-June, 1980. Original article submitted July 11, 1979.

0021-8944/80/2103-0339 $07.50

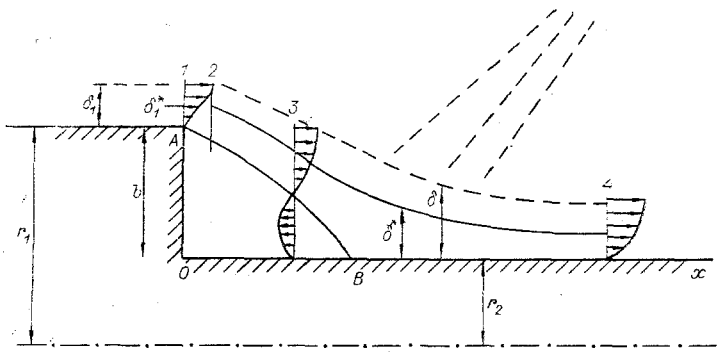

Fig. 1

$$\rho u\frac{\partial u}{\partial x}+\rho v\frac{\partial u}{\partial y}=-\frac{\partial p}{\partial x}+\frac{\partial\left(\mu\frac{\partial u}{\partial y}\right)}{\partial y}; \tag{1.2}$$

$$\rho u\frac{\partial I}{\partial x}+\rho v\frac{\partial I}{\partial y}=u\frac{\partial p}{\partial x}+\mu\left(\frac{\partial u}{\partial y}\right)^2+\frac{\partial}{\partial y}\left(\frac{\mu}{\mathrm{Pr}}\frac{\partial I}{\partial y}\right) \tag{1.3}$$

with the boundary conditions

$$\text{for}\quad y=0\quad u=v=0,\ I=I_w,$$
$$\text{for}\quad y=\delta\quad u=u_1,\quad I=I_1,$$

where I is the enthalpy; μ is the dynamic viscosity; Pr is the Prandtl number; the subscript 1 refers to parameters at the outer edge of the boundary layer; and the subscript w refers to parameters at the wall.

The boundary conditions at the initial section of the interaction region 3 are the relations obtained from the conditions for conservation of mass, momentum, and energy at the boundary of the constant-pressure flow zone and the interaction region. For the boundary conditions at the final section 4, for the system of equations (1.1)-(1.3) applied in calculating the flow in the interaction region, we take the conditions written for a zero-gradient laminar boundary layer (the pressure gradient parameter f = 0; the angle between the velocity vector at the edge of the boundary layer and the body surface $\beta = 0$). It should be noted that in the interaction region behind the obstacle ($x < x_4$) both of these parameters f and β differ from zero, and $\beta < 0$.

Applying the Stewartson–Dorodnitsyn transformation

$$\xi=\int_0^x\lambda^*\frac{p_1}{p_{01}}\frac{a_1}{a_{01}}\,ds,\quad \eta=\frac{a_1}{a_{01}}\int_0^n\frac{\rho}{\rho_{01}}\,dn, \tag{1.4}$$

we reduce the system of equations for the compressible boundary layer to a system of boundary-layer equations for incompressible flow; here it is assumed that C_p = const and Pr = 1, and

$$\frac{\mu}{\mu_{01}}=\lambda^*\frac{I}{I_{01}},\quad \lambda^*=\sqrt{\frac{I_w}{I_{01}}}\left(\frac{I_{01}+C}{I_w+C}\right),$$

where C is the Sutherland constant.

From the system of equations for the incompressible boundary layer we can obtain the following integral equation [2, 3]:

$$\frac{d\theta^{**}}{d\xi}+\frac{1}{U_1}\frac{dU_1}{d\xi}(2\theta^{**}+\theta^*)=\frac{\nu_{01}}{U_1^2}\left(\frac{\partial U}{\partial\eta}\right)_w. \tag{1.5}$$

Here $U = (a_{01}/a_1)u$ is the velocity in the transformed coordinate system

$$\theta^*=\int_0^\theta\left(1-\frac{U}{U_1}\right)d\eta,\quad \theta^{**}=\int_0^\theta\frac{U}{U_1}\left(1-\frac{U}{U_1}\right)d\eta, \tag{1.6}$$

where θ, θ^*, θ^{**} are, respectively, the boundary-layer thickness, the displacement thickness, and the momentum loss thickness for the incompressible boundary layer.

We introduce the notation $S = I_0/I_{01} - 1$, where I_0 is the stagnation enthalpy. We introduce the parameters

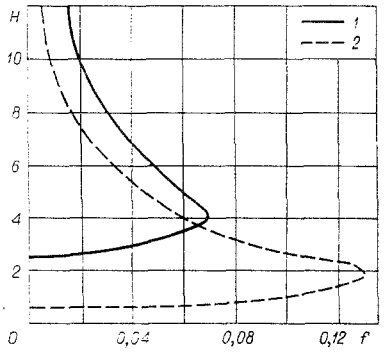

Fig. 2

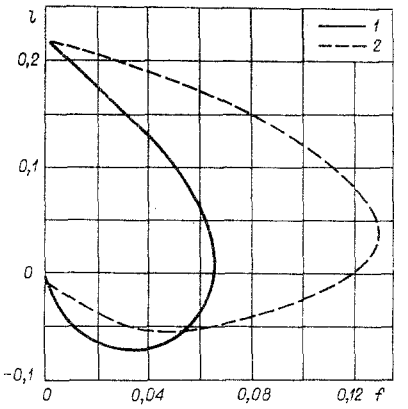

Fig. 3

$$l = \frac{\theta^{**}}{U_1}\left(\frac{\partial U}{\partial \eta}\right)_w, \quad f = -\frac{\theta^{**2}}{\nu_{01}}\frac{\partial U_1}{\partial \xi}, \tag{1.7}$$
$$F = 2[f(H+2) + l], \quad H = \theta^*/\theta^{**}, \quad h = \delta^*/\delta^{**}.$$

From the second relation of Eq. (1.7) we can obtain the expression

$$dM/dx = -f\xi^0 M/\theta^{**}\mathrm{Re}_*,$$

where $\xi^0 = d\xi/dx$; $\mathrm{Re}_* = U_1\theta^{**}/\nu_{01}$. From Eqs. (1.5) and (1.7) we also obtain

$$d\theta^{**}/dx = F\xi^0/2\mathrm{Re}_*.$$

Since the outer edge of the boundary layer intersects a stream line of the perfect fluid at a local angle whose tangent is $d\delta/dx - \tan\beta$, the continuity equation is written in the form [1]

$$\frac{d\delta}{dx} - \operatorname{tg}\beta = \frac{1}{\rho_1 u_1}\frac{dm}{dx} \quad \left(m = \int_0^\delta \rho u dy\right),$$

where β is the angle between the velocity vector at the edge of the boundary layer and the x axis. After transformations we obtain

$$\frac{d\delta^*}{dx} = \operatorname{tg}\beta + \frac{\delta^*}{\rho_1 u_1}\left(\frac{1}{h^*} - 1\right)\frac{d(\rho_1 u_1)}{dx},$$

where δ, δ^*, δ^{**} are the boundary layer thickness, the displacement thickness, and the momentum loss thickness of the compressible boundary layer; $h^* = \delta^*/\delta$; $H^* = \theta^*/\theta$.

Thus, the system of equations determining the flow in the zone of interaction of the boundary layer and the external perfect flow has the form

$$dM/dx = F_0(M, \delta^*, \theta^{**}), \quad d\delta^*/dx = \varphi = F_1(M, \delta^*, \theta^{**}),$$
$$d\theta^{**}/dx = F_2(M, \delta^*, \theta^{**}). \tag{1.8}$$

where

$$F_0 = -\frac{f\xi^0 M}{\theta^{**}\mathrm{Re}_*}; \quad F_1 = \operatorname{tg}\beta + \frac{\delta^*}{F_3}F_3'\left(\frac{1}{h^*} - 1\right)\frac{dM}{dx};$$
$$F_2 = \frac{F\xi^0}{2\mathrm{Re}_*}; \quad F_3 = M\frac{p_1}{p_{01}}\frac{a_{01}}{a_1}; \quad \varphi = \frac{d\delta^*}{dx}.$$

In order to use the system (1.8) we need to find the relation between the parameters H, H*, l, F, S_w and f. We can find these by using the Falkner–Skan similarity solutions for gradient laminar flows in an incompressible boundary layer, obtained in [2, 3]. Figures 2-4 show the computed relations thus obtained H = H(f), $l = l$(f) and H* = H*(H) for $S_w = 0$ and -0.8, which determine the relations for the incompressible boundary layer between the shape factor H and the pressure gradient parameter f, between the friction parameter l and the parameter f, and also $H^* = \theta^*/\theta$ and H. Here subscript 1 denotes curves with $S_w = 0$, and subscript 2 denotes curves with $S_w = -0.8$. The curves in Figs. 2 and 3 have two solution branches, corresponding to attached and separated flow. In Fig. 2 the attached flow region corresponds to

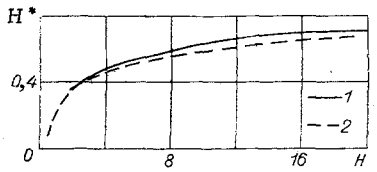

Fig. 4

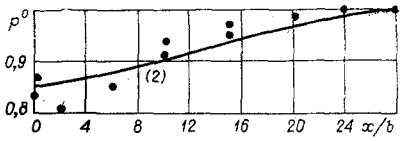

Fig. 5

the lower branch of the curve, and the separated flow corresponds to the upper branch. In Fig. 3, on the other hand, the upper branch of the curve defines the attached flow region, and the lower branch defines the separated region. With variation of S_w there is a change in the shape of the curves, and there is a change in the location of the points of boundary-layer attachment and separation.

In order to solve the system (1.8) we must relate the basic parameters of the physical flow plane and the transformed flow plane. Using Eqs. (1.4), (1.6), and (1.7), we obtain

$$\xi^0 = \lambda^* \frac{p_1}{p_{01}} \frac{a_1}{a_{01}}; \tag{1.9}$$

$$\delta^{**} = \theta^{**} \frac{\rho_{01}}{\rho_1} \frac{a_{01}}{a_1}; \tag{1.10}$$

$$h = \frac{I_{01}}{I_1} H + \left(\frac{I_{01}}{I_1} - 1 \right); \tag{1.11}$$

$$h^* = \frac{HI_{01}/I_1 + 0{,}5\,(\varkappa - 1)\,M^2}{H/H^* - 0{,}5\,(\varkappa - 1)\,M^2\,(H+1)}, \tag{1.12}$$

where

$$H = (\theta^* + S_w\theta_T^*)/\theta^{**}; \quad \theta_T^* = \int_0^\theta S d\eta / S_w.$$

At each step during the computations, in integrating the system of equations (1.8) we determine the parameters M, δ^*, θ^{**} and find the momentum loss thickness δ^{**} from Eq. (1.10). Then we calculate the additional boundary layer parameters H, H*, h, h*, f, l. Here $h = \delta^*/\delta^{**}$; the parameter H is calculated from Eq. (1.11), and then we find f from H using Fig. 2, and the value of l is determined from Fig. 3. The parameter H* is determined from Fig. 4, and the parameter h* is calculated from Eq. (1.12). For planar flow the parameter β is computed from the Prandtl–Meyer relation, and by the method of characteristics for axisymmetric flow.

2. The initial conditions for the system of equations (1.8), describing the flow in the interaction zone in the wake behind the obstacle, are determined from the condition that this flow must match the flow in the constant-pressure mixing zone.

We shall denote by δ_1, δ_1^*, δ_1^{**}, M_1, respectively, the boundary-layer thickness, the displacement thickness, the momentum loss thickness, and the Mach number. Considering first planar flow, we assume that at section 2, corresponding to rotation of the external perfect flow through an angle $\beta_2 = \lambda(M_1) - \lambda(M_2)$, a boundary layer arises with parameters δ_2, δ_2^*, δ_2^{**}, M_2. The relation between the parameters δ_1^{**} and δ_2^{**} for the boundary layer which has passed through the expansion wave, we shall choose in the form [13]

$$\delta_2^{**}/\delta_1^{**} = z = (\rho_1 u_1 M_1^2)_1/(\rho_1 u_1 M_1^2)_2. \tag{2.1}$$

We determine the parameters in the constant pressure flow zone. From the second relation of Eq. (1.8) we calculate the displacement thickness δ_-^*, and then, using the conditions for conservation of mass and momentum in the constant-pressure zone, we determine the momentum loss thickness

$$\delta_-^* = (\delta_1^* + b) + \varphi_- x, \quad \delta_-^{**} = \delta_2^{**}, \quad \varphi_- = \operatorname{tg} \beta_2 \,(M_- = M_2). \tag{2.2}$$

Matching of the interaction flow with the constant-pressure flow is done, as in [14], with the condition for conservation of the displacement thickness and the momentum loss thickness at section 3:

$$\delta_{3-}^* = \delta_{3+}^*, \quad \delta_{3-}^{**} = \delta_{3+}^{**}. \tag{2.3}$$

We determine the length of the constant-pressure region x_3 from the condition that the velocity and enthalpy should be the same on the dividing streamline of the mixing zone and on the dividing streamline in the interaction region at section 3:

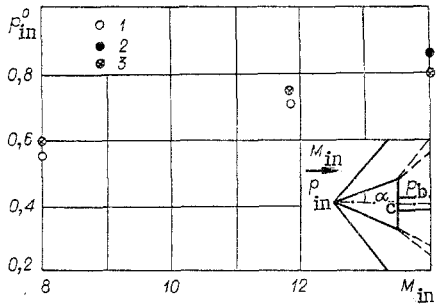

Fig. 6

$$a^*_{3-} = a^*_{3+}, \quad I^0_{3-} = I^0_{3+}; \tag{2.4}$$

where $a^* = U_*/U_1$; $I^0 = I^*_0/I_{01}$; U_* and I^*_0 are the velocity and total enthalpy on the dividing streamline.

In the flow interaction region, using the Falkner–Skan similarity solutions, we can obtain the relation $H = H(a^*, I^0)$, which it is convenient to represent, for $I_w/I_{01} = 1$ (here $I^0 = 1$) in the form [4, 5]

$$H = (0.248 - 0.435a^* - 0.0366a^{*2})^{-1}. \tag{2.5}$$

We now choose a dimensionless coordinate for the constant-pressure mixing zone in the form

$$x^* = \frac{X}{\delta_1^{**}} \frac{1}{\mathrm{Re}} = \frac{1}{\mathrm{Re}^*}, \tag{2.6}$$

where

$$X = x_3/\cos\beta_2; \quad \mathrm{Re} = \rho_1 u_1 X/\mu_1; \quad \mathrm{Re}^* = \rho_1 u_1 \delta_1^{**}/\mu_1.$$

We can calculate the relative velocity a^* as a function of x^* and I^0 for the mixing zone by the method of [6, 7]. For the case $I^0 = 1$ the dependence of a^* on x^* has the form [6]

$$a^* = 0.338 + 0.278 \lg x^*. \tag{2.7}$$

By simultaneous use of Eqs. (2.1)-(2.7) we can determine the length x_3 and calculate the parameters δ_3^*, δ_3^{**}, M_3, which serve as initial boundary conditions for integrating the system of equations (1.8). Here from the given M_2 we determine β_2, and from Eqs. (2.1) and (2.2) we calculate δ_3^{**} and φ_3. From the known value of δ_1^{**} we calculate Re^*, and from Eq. (2.6) we calculate x^*. From Eqs. (2.7) and (2.5) we calculate the shape factor H_3 and then h_3 from Eq. (1.11). Using the value of h_3, we can calculate the displacement thickness $\delta_3^* = h_3\delta_3^*$. For section 3 we write the first relation of Eq. (2.2) in the form

$$x_3 = \delta_3^{**}\left(h_3 - \frac{\delta_1^* + b}{\delta_3^{**}}\right)\Big/\varphi_3. \tag{2.8}$$

From Eq. (2.8) we find x_3, since all the quantities on the right side are known.

The flat plate flow conditions ($\beta_4 = 0$, $f_4 = 0$) serve as the final boundary conditions at section 4. We note that the calculation is simplified for $\delta_1 \geqslant b$. In that case boundary layer flow is realized practically everywhere behind the obstacle and $x_3 \approx 0$. In solving the boundary problem, as in [14], for the system of equations (1.8) the integration is done from section 3 in the direction of the main flow, up to section 4; here the value of M_2 (or of p_2) is chosen by a "ranging" method in such a way as to obtain the parameters $\beta_4 = 0$ and $f_4 = 0$ at section 4.

3. For laminar flow behind the obstacle, as has been shown by experimental investigations [8, 9], the governing parameters are M_1, Re, δ_1^{**}/b, S_w. We consider the influence of these on the base pressure. Calculations show that with increase of M_1 there is a decrease in the base pressure, a decrease in Re leads to an increase in base pressure, an increase in the relative boundary-layer thickness increases the base pressure, and cooling of the obstacle surface (decrease in S_w) reduces the base pressure. To find the influence of S_w on the base pressure we performed calculations for $S_w = 0$ and -0.8 for the case where the boundary-layer thickness is comparable with the obstacle height ($\delta_1 \approx b$).

Figure 5 shows the calculated pressure distribution $p^0 = p/p_1$ behind the obstacle at $M_1 = 2.9$ for the undisturbed flow ahead of the obstacle (solid curve), and compares this with experimental data (points) corresponding to the values $M_1 = 2.9$, $\mathrm{Re}_1 = 0.3 \cdot 10^5$, $b = 0.2 \cdot 10^{-2}$ m for which the experiments were conducted.

An annular contoured nozzle with a center-body was used in the experiment. The center-body was a model, a cylinder with an axisymmetric step whose surface was parallel to the flow axis. The model diameter ahead of the step was $d = 2r_1 = 20$ mm, and the step height was $b = 2$ mm. The static pressure was measured ahead of the step and along the surface behind the step, using tubes with internal diameter $d_1 = 0.8$ mm. The Reynolds number Re_1 was computed for the incident flow ahead of the step, using the center-body length from the nozzle throat to the base. To measure the static pressure we used manometers filled with a liquid of low specific gravity and low vapor pressure (dibutylphthalate, specific gravity 1.049 g/cm^3, vapor pressure 10^{-6} torr). Prior to the experiment a fore-vacuum pump evacuated the manometer cavities and tank to 10^{-2} torr. The error in measuring the base pressure was 2-4%. The value of M at the nozzle exit was calculated from the total profiles in the core. The asymmetry in p_0'/p_0 within the core ($y \approx 2$-12 mm) was $\Delta(p_0'/p_0) \approx 7\%$, which corresponds to a variation of $M \sim 1\%$.

The boundary-layer thickness ahead of the separation ($\delta_1 \approx 2.2$ mm) was measured by means of a total pressure tube (a micro-probe); here we determined the boundary between the annular flow core and the boundary layer. We used this approach because the investigations were done at low pressures and the accuracy in measuring the p_0'/p_0 profile was low.

Estimates were made of the influence of the parameter $\delta_1/r_1 \approx 0.22$ on the characteristics of the boundary layer on the convex axisymmetric surfaces, and these showed that the boundary layer before separation in the case considered is close to a flat plate boundary layer, and that some inaccuracy in determining δ_1^{**}/b has practically no influence on the base pressure. When there is flow separation on a body with $r_1 = 10$ mm, three-dimensional effects may influence the base pressure, due to differences in the flow considered from the planar case. However, as is shown by the experimental investigations of various authors, e.g., [8], this influence is small, even when significant three-dimensional effects are present in the base region.

We also computed flows behind axisymmetric steps. Here we used the same flow model as for the planar flow, but the computation of the external perfect flow (to obtain the parameter β) was done by the method of characteristics [14, 15]. To determine the parameters at section 3 of the beginning of interaction of the boundary layer with the external perfect flow we used the relations

$$\delta_3^* = (\delta_1^* + b) + \int_0^{x_3} \operatorname{tg} \beta dx, \quad \delta_3^{**} = \frac{r_1}{r_2} z \delta_1^{**},$$

which can be obtained, for the constant pressure flow zone, from the second and third equations of Eq. (1.8). The final boundary conditions for the system (1.8) are the conditions $\beta_4 = 0$ and $f_4 = 0$ at section 4. This method was applied for a base support bracket radius of $r_2 \gg \delta_1$. The results from this method of computation are compared with the results of experiments performed in [10, 11] for incident stream values of $M_{incident}$ ($M_{incident} = 8$; 11.8; 14) and of $Re_{incident}$ based on the model midsection diameter and the incident stream parameters of $Re_{cone} = 2.5 \cdot 10^5$; $5 \cdot 10^5$; $0.12 \cdot 10^5$. In these experiments the base pressure $p^0_{incident} = p_{base}/p_{incident}$ was measured behind cones of semivertex angle $\alpha_c = 5°$ [10] and 15° [11]. The experimental results are shown in Fig. 6 by points 1 and 2, respectively, for [10] and [11], and points 3 show the calculations done for flow over the cones. In the computations we used the relation

$$p^0_{in} = \frac{p_b}{p_c} \frac{p_c}{p_{in}},$$

where $p_{incident}$ is the pressure in the oncoming stream; p_{cone}, p_{base} are the pressures on the cone surface and in the base region. The ratio $p_{cone}/p_{incident}$ was calculated for a given $M_{incident}$ from conical flow tables, and the ratio p_{base}/p_{cone} was calculated using the method of this paper. The calculation was done for a cone with a base bracket whose relative size is $r_2/r_1 = 0.25$. The experimental results on base pressure behind a cylindrical body and a cone with a base bracket, for turbulent, transitional, and laminar flow conditions [12, 16] show that the base pressure for $r_2/r_1 = 0$–0.3 is approximately constant. Therefore, we can compare the calculated results for $r_2/r_1 = 0.25$ with the experimental data for $r_2/r_1 = 0$. The results of the calculations (Fig. 6) show satisfactory agreement with experiment.

LITERATURE CITED

1. L. Crocco and L. Lees, "Mixing theory to determine the interaction of dissipative and almost isentropic flows," Vopr. Raketn. Tekh., No. 2 (1953).
2. C. B. Cohen and E. Reshotko, "Similar solution for the compressible laminar boundary layer with heat transfer and pressure gradient," NACA Rep. No. 1293 (1956).
3. C. B. Cohen and E. Reshotko, "The compressible laminar boundary layer with heat transfer and arbitrary pressure gradients," NACA Rep. No. 1294 (1956).
4. V. Reeves and L. Lees, "Supersonic separated and attached laminar flows. Part 1. General theory and its application to analysis of interaction between a shock and an adiabatic boundary layer," Raketn. Tekh. Kosm, No. 11 (1964).
5. L. Lees and V. Reeves, "Theory of the laminar near wake behind blunt bodies in hypersonic flow," Raketn. Tekh. Kosm., No. 11 (1965).
6. M. Denison and E. Baum, "Compressible free shear layer with finite initial thickness," AIAA J., No. 1 (1963).
7. R. Page and R. Dickson, "Transformation in the wake problem," Raketn. Tekh. Kosm., No. 8 (1964).

8. R. White, "Laminar separation and reattachment behind a downstream-facing step at hypersonic Mach number, including the effect of the approach boundary layer," Medd. Flygtekn. Föröksanst, No. 103 (1956).
9. D. Chapman, D. Kuehn, and H. Larson, "Investigation of separated flow in supersonic and subsonic streams with emphasis on the effect of transition," NACA Rep. No. 1356 (1958).
10. Zakkay and Cresci, "Experimental investigation of the near wake behind a slender cone at M = 8 and 12," Raketn. Tekh. Kosm., No. 1 (1966).
11. L. Lokman, Measurement of the base pressure and the heating in flow over blunt and sharp cones in a shock tube, Raketn. Tekh. Kosm., No. 10 (1967).
12. D. Chapman, "Analysis of base pressure at supersonic velocities and comparison with experiment," NACA Rep. No. 1051 (1951).
13. J. E. Nash, "An analysis of two-dimensional turbulent base flow, including the effect of the approaching boundary layer," ARC RM No. 3344 (1963).
14. A. N. Antonov, "Calculation of the interaction of a turbulent boundary layer with the external supersonic flow behind an obstacle," Izv. Akad. Nauk SSSR, Mekh. Zhidk. Gaza, No. 3 (1971).
15. A. N. Antonov, "Calculation of the interaction of a turbulent boundary layer with the external supersonic flow in a concave corner and on the spherical base part of the body," Zh. Prikl. Mekh. Tekh. Fiz., No. 1 (1976).
16. S. Donaldson, "The effect of sting supports on the base pressure on a blunt-base body in a supersonic stream," Aeron. Quart., 6, No. 2 (1955).

SOLITONS IN A DOWN-FLOWING FILM WITH MODERATE MASS FLOW RATES OF THE LIQUID

O. Yu. Tsvelodub

UDC 532.51

Using the hypothesis of self-similarity, in [1] an equation was obtained describing long-wave perturbations in a vertical film of liquid with moderate mass flow rates:

$$\left(\frac{\partial}{\partial t}+3\frac{\partial}{\partial x}\right)h+6h\frac{\partial h}{\partial x}-\frac{2}{15}\mathrm{Re}\frac{\partial}{\partial t}\left(h\frac{\partial h}{\partial t}\right)+\frac{\mathrm{Re}}{3}\left(\frac{\partial}{\partial t}+1.69\frac{\partial}{\partial x}\right)\left(\frac{\partial}{\partial t}+0.71\frac{\partial}{\partial x}\right)h+\mathrm{W}\frac{\partial^4 h}{\partial x^4}=0, \tag{1}$$

where $\mathrm{Re}=gh_0^3/3\nu^2$; $\mathrm{W}=\sigma/\rho h_0^2$; h is the shift of the surface of the film from the unperturbed level, measured in units of h_0; and h_0 is the thickness of the unperturbed film.

For a steady-state running wave h = h(x − ct), from (1) we obtain

$$(3-c)h'+6hh'-2\ \mathrm{Re}\ c^2(hh')'/15+\mathrm{Re}(1.69-c)(0.71-c)h'''/3+\mathrm{W}h^{\mathrm{IV}}=0 \tag{2}$$

(a prime means differentiation with respect to x).

In finding soliton solutions of Eq. (2), it can be integrated once:

$$(3-c)h+3h^2-2\,\mathrm{Re}\,c^2hh'/15+\mathrm{Re}\,(1.69-c)(0.71-c)h'/3+\mathrm{W}h'''=0. \tag{3}$$

Using the replacement

$$\begin{gathered}h=aH,\ x_1=bx,\\ a=\mathrm{W}b^3,\ b=(\mathrm{Re}(1.69-c)(0.71-c)/3\mathrm{W})^{1/2}\end{gathered} \tag{4}$$

Eq. (3) is brought to the form

$$-c_1H+3H^2-2mHH'-H'+H'''=0, \tag{5}$$

where

$$\begin{gathered}c_1=(c-3)(3(z(1.69-c)(0.71-c)))^{6/5},\\ m=c^2z((1.69-c)(0.71-c)/3)^{1/2}/15,\ z=(\mathrm{Re}^3/\mathrm{W})^{1/2}.\end{gathered} \tag{6}$$

Relationships (4)-(6) are valid if

$$c>1.69\quad\text{or}\quad c<0.71.$$

Novosibirsk. Translated from Zhurnal Prikladnoi Mekhaniki i Tekhnicheskoi Fiziki, No. 3, pp. 64-66, May-June, 1980. Original article submitted June 22, 1979.

0021-8944/80/2103-0345 $07.50